Meteoritics & Planetary Science 40, Nr 3, 397–408 (2005)
Abstract available online at http://meteoritics.org

Evidence of space weathering in regolith breccias I: Lunar regolith breccias

Sarah K. NOBLE,[1*] Lindsay P. KELLER,[2] and Carlé M. PIETERS[1]

[1]Department of Geological Sciences, Brown University, Box 1846, Providence, Rhode Island 02912, USA
[2]NASA Johnson Space Center, Mail Code SR, Houston, Texas 77058, USA
*Corresponding author. E-mail: noble@porter.geo.brown.edu

(Received 14 May 2004; revision accepted 9 February 2005)

Abstract–We have analyzed a suite of lunar regolith breccias in order to assess how well space weathering products can be preserved through the lithification process and therefore whether or not it is appropriate to search for space weathering products in asteroidal regolith breccia meteorites. It was found that space weathering products, vapor/sputter deposited nanophase-iron-bearing rims in particular, are easily identified in even heavily shocked/compacted lunar regolith breccias. Such rims, if created on asteroids, should thus be preserved in asteroidal regolith breccia meteorites. Two additional rim types, glass rims and vesicular rims, identified in regolith breccias, are also described. These rims are common in lunar regolith breccias but rare to absent in lunar soils, which suggests that they are created in the breccia-forming process itself. While not "space weathering products" in the strictest sense, these additional rims give us insight into the regolith breccia formation process. The presence or absence of glass and/or vesicular rims in asteroidal regolith breccias will likewise tell us about environmental conditions on the surface of the asteroid body on which the breccia was created.

INTRODUCTION

The term "space weathering" refers to the cumulative effects of several processes operating at the surface of any solar system body not protected by a thick atmosphere. These processes include cosmic and solar ray irradiation, solar wind implantation, and sputtering, as well as micrometeorite bombardment, which can dramatically alter the visible and near infrared (Vis/NIR) spectral properties of surfaces observed using remote-sensing techniques (Pieters et al. 1993). Our understanding of the processes and products of space weathering comes almost exclusively from studies of lunar samples (e.g., Keller and McKay 1993, 1997; Pieters et al. 2000; Hapke 2001 and references therein; Wentworth et al. 1999; Bernatowicz et al 1994). In lunar soils, the most voluminous weathering products are agglutinates, that is, glass welded aggregates created via micrometeorite bombardment. These agglutinates comprise up to 60 vol% of a mature lunar soil (McKay et al. 1991). In terms of surface area, however, the finer particles dominate the optical properties of lunar soils (Noble et al. 2001b). Space weathering produces thin (60–200 nm), amorphous rims surrounding individual grains in mature soils. Many of these rims result from the deposition of impact-generated vapors or sputtered material and are characterized by inclusions of nanophase iron ($npFe^0$). These nanometer-scale inclusions of metallic iron are also observed in agglutinitic glass. The abundance and distribution of $npFe^0$ is the primary cause of spectral alteration of lunar soils (see review in Hapke 2001). They contribute to the characteristic "space weathering continuum" of lunar soils (Noble et al. 2001b) and result in the observed "darkening" and "reddening" of the Vis/NIR spectral region (Pieters et al. 2000).

While the case for space weathering is now generally accepted for the Moon, it is not clear if these results can be extrapolated to other solar system bodies such as asteroids. Only a few classes of meteorites can be directly related to asteroid families through remotely sensed data, and the most abundant class of meteorites (the ordinary chondrites) do not have spectral properties comparable to asteroids. It has been suggested that the development of $npFe^0$ (space weathering) can account for the discrepancies (Pieters et al. 2000). Space weathering is likely dependent on many variables (e.g., surface composition, distance from the Sun, micrometeorite flux, etc.) and so its products are expected to vary from body to body. We do not yet fully understand the details of how space weathering manifests itself on asteroids or how the products of asteroidal space weathering will affect remotely sensed data.

Unlike the Moon, no direct samples of unconsolidated asteroidal surface regolith are available for study. The only near-surface asteroid samples currently available are a class

Table 1. Lunar regolith breccia samples used in this study.

Sample #	Sample type[a]	SEM	TEM	Friability[b]
10068	GM	√	√	2
10068	chip	√		2
10068	TS	√	√	2
15505	TS	√	√	4
79035	TS	√	√	1
79035	chip	√		1
QUE 93069	TS	√		5

[a]TS = thin section; GM = grain mount; chip = fresh chip.
[b]Friability is ranked from 1 to 5, with 1 being most friable and 5 the most competent.

of meteorites known as "regolith breccias," or "gas-rich" meteorites that show evidence of surface exposure. These meteorites, composed of consolidated rock fragments and soil, are characterized by high concentrations of solar-wind-implanted gases, indicating that many constituent grains have been directly exposed to the space environment (i.e., as regolith on an asteroid body). Can we use these rocks as a proxy for asteroidal regolith? What, if any, changes occur to space weathered materials when unconsolidated/loose regolith is lithified into rock? Are the products of space weathering such as amorphous rims and agglutinates preserved? Are other types of grains or coatings produced that are unique to regolith breccias? To answer these questions and to gain insight into the regolith breccia forming process, we have undertaken a detailed optical and electron microscopy study of a suite of lunar regolith breccias showing a range of friability/lithification/compaction/shock features and space weathering extent. In the lunar case, we have surface regolith (soils) for direct comparison. The results of this investigation with lunar materials will provide a baseline for comparison to similar analyses of meteorite regolith breccias (Noble et al. Forthcoming).

METHODS AND SAMPLES

We studied a total of eight lunar regolith breccia samples and selected a subset of four samples (79035, 10068, 15505, and QUE 93069) for detailed analysis. These four samples and the analytical tools utilized for each are listed in Table 1. These samples span a wide range of petrographic textures, from friable, porous, poorly lithified breccia 79035 to highly consolidated, low porosity QUE 93069 (Fig. 1). Petrographic thin sections were first examined using a petrographic microscope followed by backscattered electron imaging and chemical analysis using a JEOL 5910 scanning electron microscope (SEM) equipped with an IXRF energy-dispersive X-ray (EDX) spectrometer. Regions of interest were extracted from the thin sections and electron transparent transmission electron microscope (TEM) specimens were prepared by ion milling. Samples of the 10068 grain mount and fragments of 79035 were embedded in epoxy and thin sections (approximately 70 nm thick) prepared using an ultramicotome. We used a JEOL 2000FX TEM equipped with a Noran EDX spectrometer and a Philips 420 TEM for the TEM observations.

The terminology applied to breccia samples varies widely. Here we follow the conventions described in Christie et al. (1973) and Bischoff et al. (1983). Breccias are classified as types A, B, or C based on textural features such as porosity, shock effects, and glass content, with type A being the most porous, least shocked, and lowest in glass content.

Lunar regolith breccia 79035 is a class A breccia, the most friable breccia examined in this study. It is a highly porous mare soil breccia with abundant agglutinates (Fruland 1983). Previous high voltage TEM studies showed that regolith products such as glass spherules and vesicular melt glass were common in this breccia and furthermore that the preservation of solar flare tracks in glass-encased mineral grains argued for rapid cooling (Heuer et al. 1974). Individual grain boundaries are easily recognized.

Lunar regolith breccia 10068 is considered a "classic soil breccia" (Fruland 1983). It is also a class A breccia. It is a coherent breccia of mature mare soil. Maturity of lunar soils are commonly measured by I_s/FeO, a measure of the amount of nanophase iron present normalized by the total iron content (Morris 1978). An immature soil has an I_s/FeO of 0–30, a submature soil an I_s/FeO of 30–60, and a mature soil an I_s/FeO of >60; an I_s/FeO breccia 10068 has an I_s/FeO of 84. This breccia is more competent and less porous than 79035. Grain boundaries are still easily recognized; in fact, the rock can be largely returned to its former soil state through freeze-thaw disaggregation (Basu et al. 2000). The disaggregated soil was found to have the same size fraction characteristics of an ordinary soil; this, in addition to TEM studies (Noble et al. 2001a; Noble et al. 2002), indicates that the breccia broke apart largely along its original grain boundaries. Grain mounts of this delithified soil were also examined via SEM and TEM.

Lunar regolith breccia 15505 has been described as moderately coherent (Fruland 1983). It has low porosity (~15%) (Warren 2001) and its matrix material has an annealed, glassy texture. Grain boundaries are much more difficult to identify in this sample. This is a class B breccia.

QUE 93069 is a feldspathic lunar highlands regolith breccia. It is an Antarctic meteorite that was chosen for its high I_s/FeO value (relative to other lunar meteorites) of 34 (Lindstrom et al. 1995). This rock is the least mature of the samples studied and should therefore contain the fewest soil rims. QUE 93069, like other lunar meteorites, has very low porosity of approximately 9% (Warren 2001). The meteorite has also been highly shocked, as evidenced by the extensive glass and recrystallized glass that composes the matrix. Similar to breccia 15505, the grain boundaries are extremely difficult to distinguish optically. Because of the large amount of shock melting, we classify this meteorite as a class C breccia.

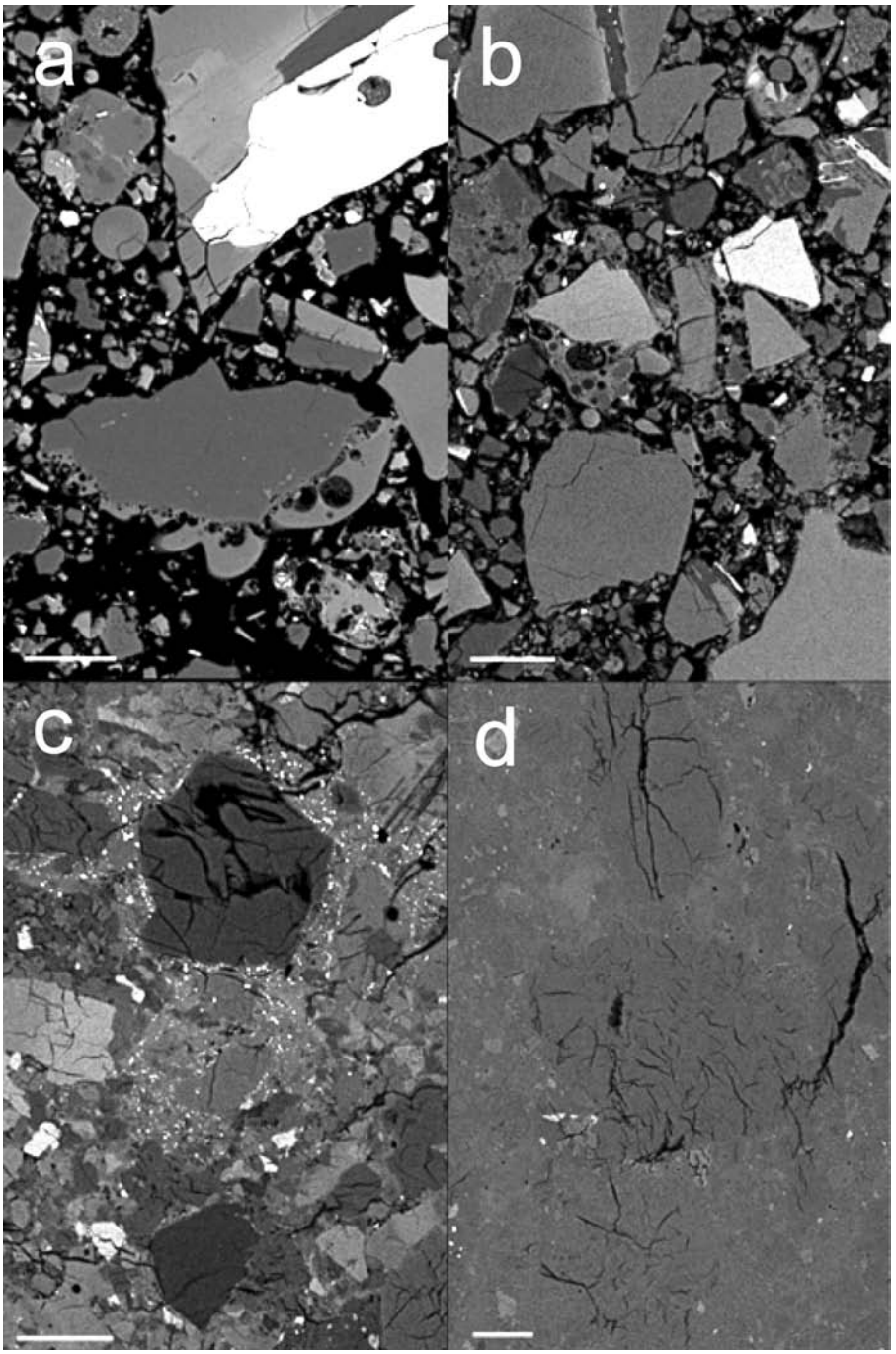

Fig. 1. SEM BSE images of lunar regolith breccia samples: a) 79035; b) 10068; c) 15505; and d) QUE 93069 (as a highland breccia, this sample is largely plagioclase and therefore displays little contrast in backscatter). Note the decreasing porosity from (a) to (d). All scale bars are 20 μm.

RESULTS AND DISCUSSION

Keller and McKay (1997) describe three distinct types of rims found on lunar soil grains: amorphous, inclusion-rich, and vesicular. In addition, compound or "multiple" rims of these aforementioned types were also found. Amorphous rims form on crystalline silicate grains in response to solar wind irradiation and have been recognized in lunar soil grains since the early 1970's (e.g., Dran et al. 1970; Borg et al. 1983). Amorphous rims show chemical evidence for preferential sputtering of constituent cations similar to effects observed in laboratory experiments (Demyk et al. 200; Carrez et al. 2002) and are thus an erosional feature of lunar grains (Keller and McKay 1997). Inclusion-rich rims, which will be referred to in this paper as nanophase-iron-bearing rims, form largely by the condensation of impact-generated vapors and sputter

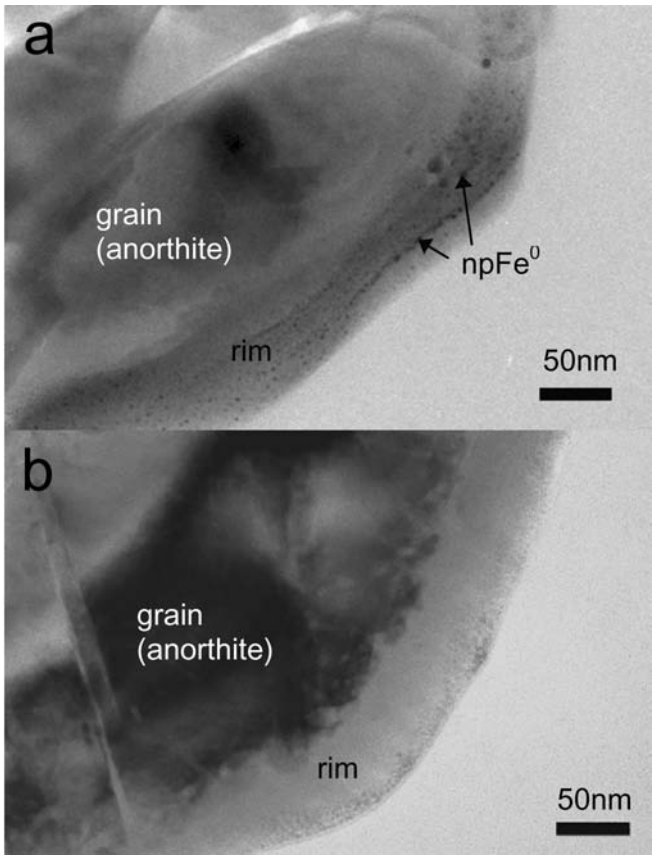

Fig. 2. a) A TEM image of a grain of lunar soil 10084 with a npFe^0-bearing-rim. b) A TEM image of a grain of lunar soil 78221 with an amorphous rim.

deposition, although the relative importance of these two processes is uncertain (Keller and McKay 1997). The nanophase-iron-bearing rims are compositionally distinct from their host grains and are a depositional feature of lunar grains. Keller and McKay (1997) noted that a continuum exists between these two major rim types in mature lunar soils. We will refer to amorphous and npFe^0-bearing rims collectively as "soil rims" because they are abundant in lunar soils and their origin is clearly linked to soil processes. Examples of these "soil" rims observed in particulate lunar soils are shown in Fig. 2. The third rim type, vesicular rims, are rare in lunar soils and their formation mechanism is poorly understood (see discussion below).

Soil Rims

Lunar regolith breccias, like their soil counterparts, contain amorphous and npFe^0-bearing rims. Both types of soil rims were identified in our breccia samples.

Soil rims are readily identified throughout the sample of 79035, the most friable breccia. One example of a npFe^0-bearing rim is shown in Fig. 3. These rims are indistinguishable from rims found in any lunar soil.

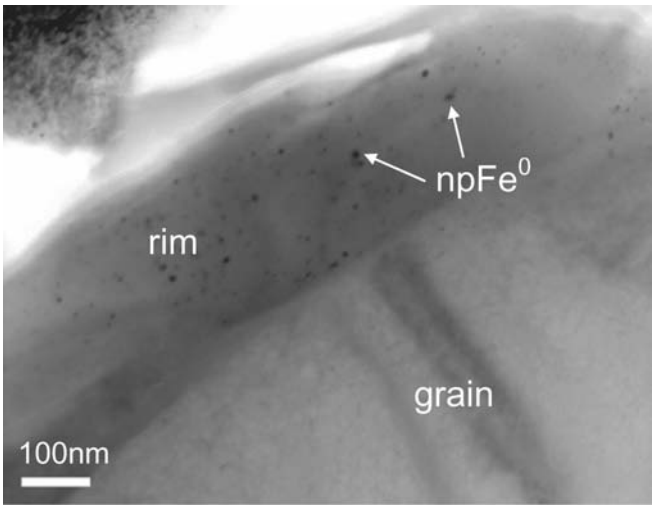

Fig. 3. A TEM bright field image of a npFe^0-bearing rim from friable lunar regolith breccia 79035.

Lithification during breccia formation does not appear to have affected the rims in any way.

Breccia 10068 was lithified from a very mature lunar soil and thus it is not surprising that of all the breccias studied, soil rims are the most common in this sample. Figure 4 is an example of a typical npFe^0-bearing rim from breccia 10068. This rim is from a sample that was prepared using delithified grains (Basu et al. 2000). These grains were embedded in epoxy and thin sections were prepared using ultramicrotomy. Like the ion-milled samples of 10068, the microtomed samples contained abundant rims of all types. Both the quantity and appearance of rims do not appear to be affected in any way by sample preparation method. Similar to what was observed in 79035, rims in 10068 are indistinguishable from those commonly found in soils and lithification does not appear to have affected these rims. Both amorphous and npFe^0-bearing rims were identified in breccia 15505. Figure 5 shows an excellent example of a multiple rim from the breccia: an amorphous rim coated with a npFe^0-bearing rim. Soil rims are much rarer here than in either 10068 or 79035. There are two possible explanations for this: either some of the rims were destroyed in the lithification process or the precursor soil for this breccia was less mature and therefore contained fewer rims initially.

If rims can be destroyed during lithification, one would also expect to find degraded rims that were only partially destroyed. In fact, while some of the rims found in 15505 are pristine and indistinguishable from rims found in any lunar soil (e.g., Fig. 5), others show evidence of having been affected by the lithification process. The rim in Fig. 6 is a good example of this degradation. While the rim is still identifiable by the distribution of npFe^0, the interface between the rim and surrounding glass is poorly defined and difficult to discern. Thus, for 15505, it is likely that some rims have been degraded to the point where they are no longer recognizable,

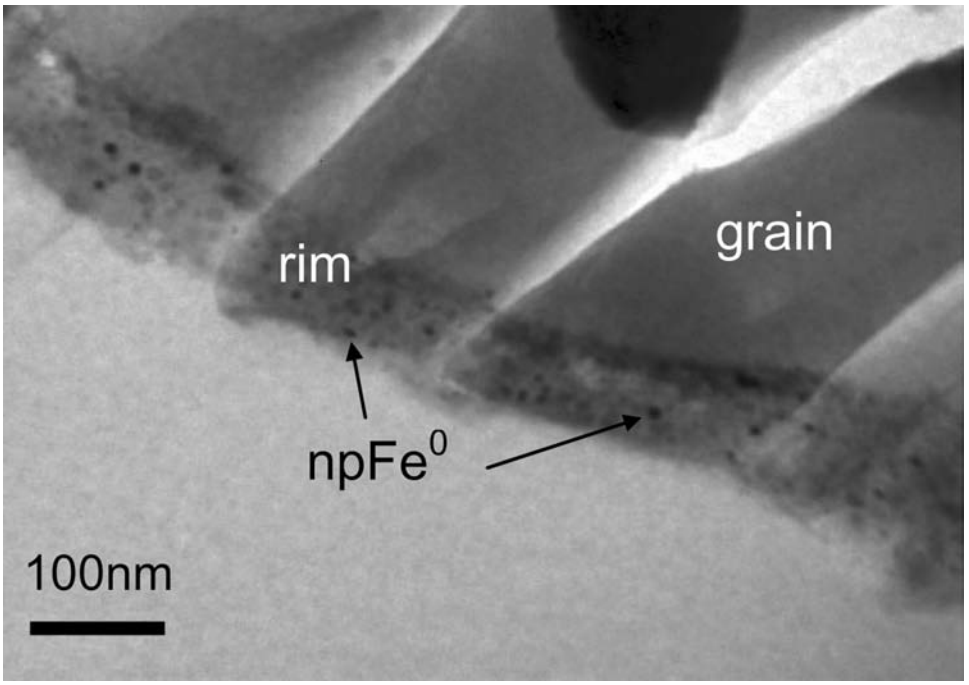

Fig. 4. A TEM bright field image of an $npFe^0$-bearing rim from the moderately coherent lunar regolith breccia 10068. The sample was prepared from a microtomed section.

though it is possible that the progenitor soil was a relatively immature soil that simply had not acquired many rims.

Breccia Rims

One of the major discoveries of this detailed analysis of breccia properties is the recognition of grain rims that appear to be generally unique to breccia samples. In addition to the soil rims described above, we found two other types of rims in the regolith breccias: vesicular and glass rims. As these rims are rare to absent in soils, we infer that they are directly related to the breccia formation process. Therefore, vesicular and glass rims will be collectively referred to as "breccia rims."

Vesicular Rims

We identified vesicular rims in all breccia samples observed using TEM. They are quite common in these breccias and are observed more frequently than soil rims. Vesicular rims range in thickness from tens of nanometers up to 1–2 micrometers. The extent of vesicular rim development is loosely correlated to size of the host grain (Fig. 7). For example, small grains in the 2–5 μm range tend to have a layer of vesicles around their entire circumference (Fig. 7a), whereas larger grains (≥5 μm) are often vesicular on only parts of their peripheries (Fig. 7b). With the smallest grains (<2 μm) it is common for the entire grain to be vesicular, not just the edges (Fig. 7c).

The major element compositions of vesicular rims are similar to their host grains. A comparison of the composition of rim material to the grain interior for a typical rim in breccia 79035 is shown in Fig. 8. We used an incident probe size that was optimized for the width of the rim, which was analyzed in order to avoid contributions from the underlying grain. Unlike vapor/sputter deposited or melt deposited rims in soils, vesicular rims appear to have formed directly from the host grain. Vesicular rims look extremely delicate, yet they seem to survive lithification very well. We see only whole and unbroken examples with few, if any, fragments or crushed rims. This makes it highly likely that they have not traveled far from their origin and suggests that they were created in situ as the rock was lithified.

The mechanism that generates the vesiculation in the rims is poorly understood, although thermal pulses and evolution of implanted solar wind gases may play an important role. Keller and McKay (1997) suggested that the few vesicular rims observed in lunar soils result from the evolution of implanted solar gases during localized heating from impacts. We believe that a similar process occurs during the formation of lunar breccias. This would allow their creation in situ and explain both their preservation, given their delicate nature, and their near-absence in lunar soils. The thermal event would have to be of sufficient strength and duration to allow the evolution of the gases, but not enough to anneal the solar flare tracks that are also common in these breccias. Both of these constraints are consistent with step-wise heating of lunar soil grains, which shows that the bulk of the solar-wind-implanted gases is evolved at temperatures <700 °C (Nier and Schlutter 1992; Nicholls et al. 1994), and from studies showing that

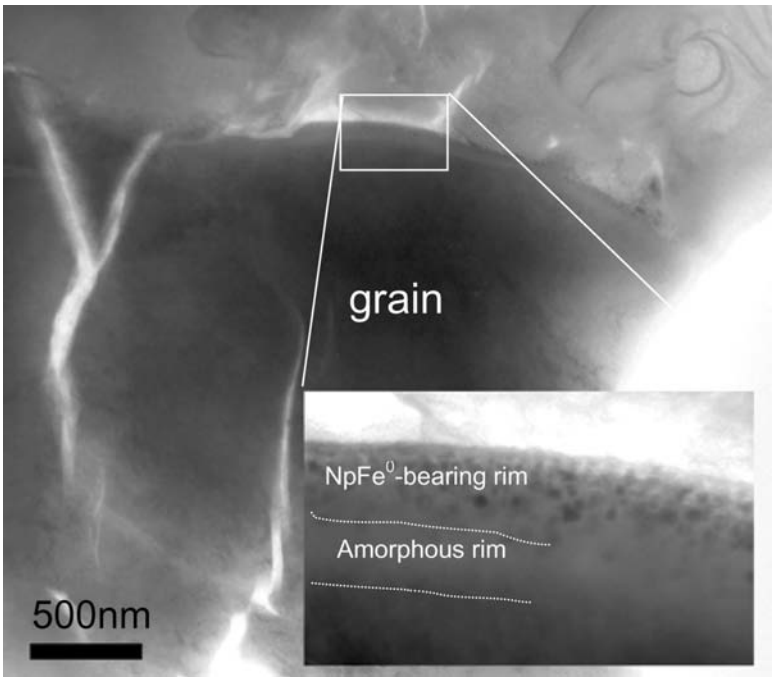

Fig. 5. A TEM bright field image of a multiple rim (amorphous + npFe^0-bearing) from the very coherent lunar regolith breccia 15505.

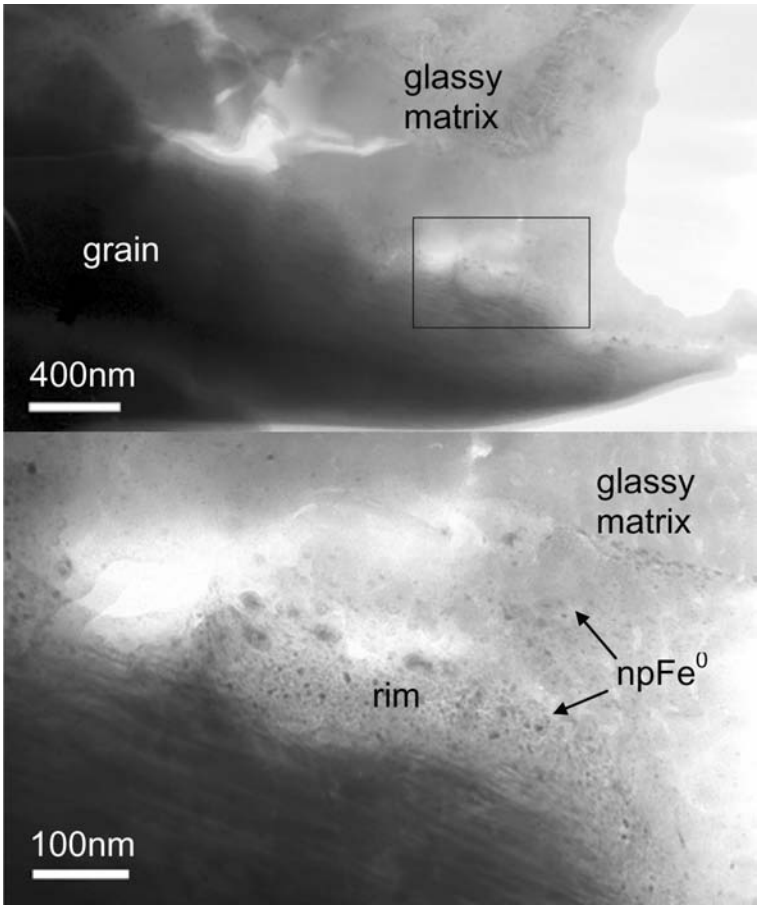

Fig. 6. a) A TEM bright field image of an npFe^0-bearing rim that is degrading into the surrounding glass; b) a close-up image of the boxed region.

solar flare tracks in minerals are erased/healed at temperatures of 650–850 °C (Fraundorf et al. 1980; Sandford and Bradley 1989). Recent experiments (Jowsiak et al. 2004) show that it is possible to generate vesicular rims on mineral grains by pulse-heating He-implanted materials, but additional experiments are required on relevant materials (plagioclase, impact glasses) to constrain the thermal history and process by which these rims form.

The vesicular rims are observed preferentially on glassy grains as compared to crystalline silicate grains. We speculate that this difference may be because the disordered structure of glass more easily allows the vesicles to form. This preference for glass is commonly seen at interfaces where glass and crystal meet (i.e., where a crystalline grain is surrounded by a glass or vapor deposited rim or where an agglutinate has incorporated crystalline grains). Under these situations it is relatively common in these breccias to see a remarkably uniform line of vesicles at the interface. Figure 9 is an example of such a vesicular line surrounding a crystalline grain within an agglutinate. The gases escape the grain without deformation, but once they reach the less ordered glass, the vesicles are nucleated.

Glass Rims

Glass rims, such as those shown in Fig. 10, are ubiquitous in lunar regolith breccias. However, like vesicular rims, glass rims are rare to absent in lunar soils. Glass rims also commonly contain vesicles, though considerably fewer than vesicular rims. They are also distinguished from vesicular rims by the presence of $npFe^0$. These rims are also distinct from the $npFe^0$-bearing soil rims that have been described previously (Keller and McKay 1997). While the $npFe^0$-bearing rims on lunar soil grains are generally ~60–200 nm thick, the glass rims are commonly much thicker (up to several micrometers in thickness). Typically, glass rims are not uniformly distributed around the host grain. The glass rims are well developed with μm-scale thickness in some places and are thin or absent in others (see especially Figs. 10c, 10d, and 10h). Commonly one can identify "flow" features that clearly indicate that the material was deposited as a melt and not a vapor (see especially Figs. 10b and 10g).

Glass rims share many characteristics with agglutinitic glass: 1) both contain vesicles that are absent in amorphous and $npFe^0$-bearing rims in soils; 2) both contain $npFe^0$ blebs that tend to be larger in diameter than the $npFe^0$ found in soil rims (e.g., Keller and Clemett 2001); and 3) both are compositionally heterogeneous on a μm-scale, but 4) their average compositions are nearly identical. Figure 11 compares the composition of glass rims and agglutinitic glass in basaltic breccia 79035 with the bulk composition data from 79035 by Wänke et al. (1975). Both the glass rims and the agglutinates are, on average, higher in Al_2O_3 and lower in FeO relative to the bulk composition. The rims, like agglutinates, are also depleted in TiO_2, which appears to indicate differential melting of soil constituents during glass formation (Pieters and Taylor 2003).

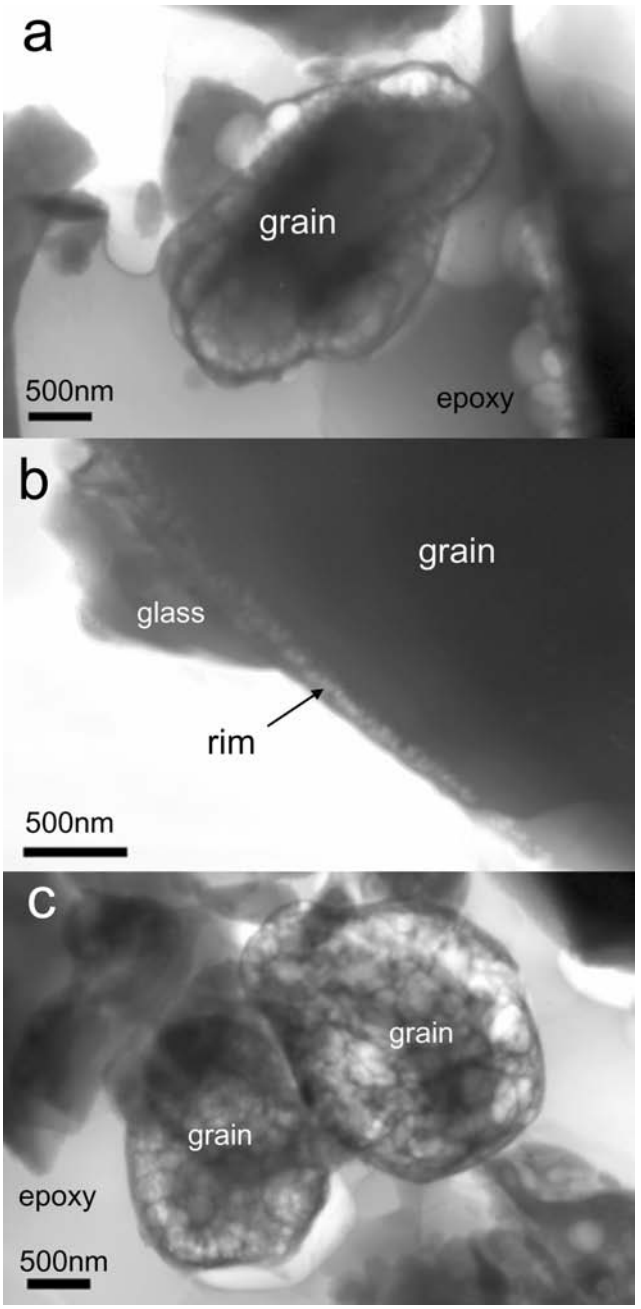

Fig. 7. Examples of vesicular rims: a) a continuous vesicular rim from 79035; b) a partially vesicular grain from 79035; c) two completely vesicular grains from 79035.

Glass rims were readily identified using both optical microscopy and SEM in all eight breccias investigated in this study. Glass rims are prominent in backscattered electron images because they are compositionally distinct from their host (in sharp contrast to the vesicular rims described above). For example, Fig. 10a is a largely plagioclase grain that

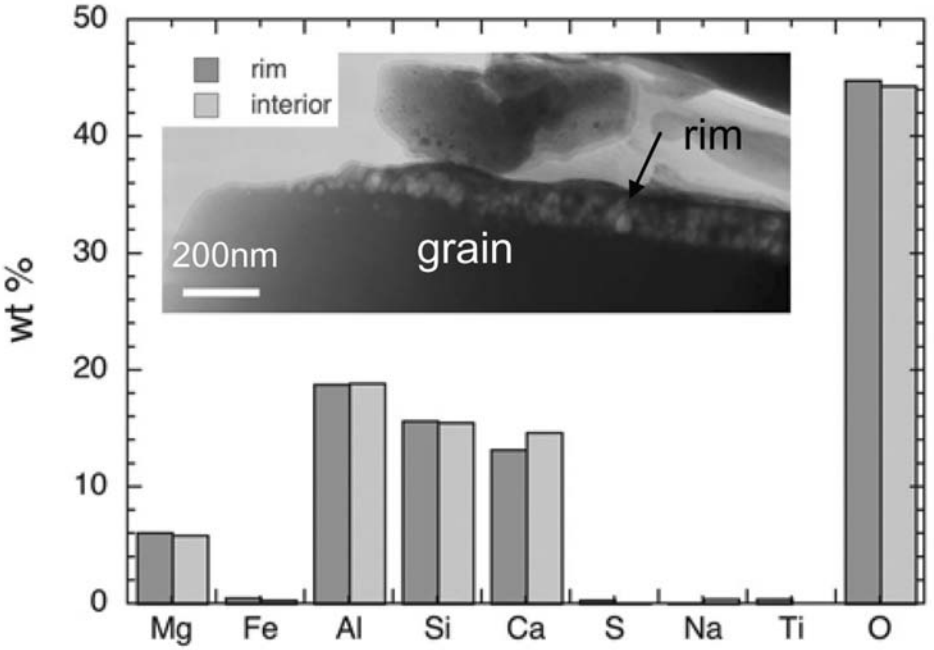

Fig. 8. This vesicular rim from 79035 is compositionally identical to the grain interior. The data are from EDX spectra.

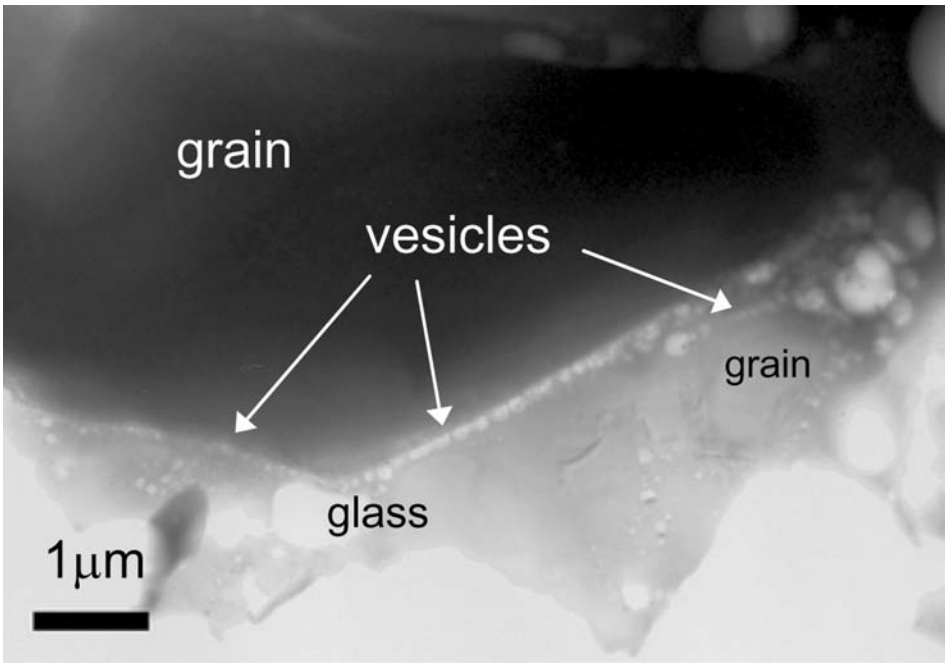

Fig. 9. A TEM bright field image of an agglutinate with imbedded grains from lunar regolith breccia 79035. A line of vesicles is often found at the interface between glass and crystal in these breccias.

appears dark in backscatter surrounded by a very bright rim. The rim contains more iron, a higher Z element, which causes it to appear brighter in backscatter. This phenomenon makes rims easier to identify in mare breccias than highland because the compositional contrast is greater. Figure 10d is an example of a highland soil glass rim. Even with the lower contrast, the rim is still slightly brighter and is distinguished by its flow texture and vesicles. Rims are also much more difficult to identify in the less porous breccias 15505 and QUE 93069 (Figs. 10e and 10f, respectively). While all samples investigated contained glass rims, the abundance of these rims varied from sample to sample. Some thin sections contained only a few rims, while in others the rims were ubiquitous with 15–20% of grains at least partially rimmed.

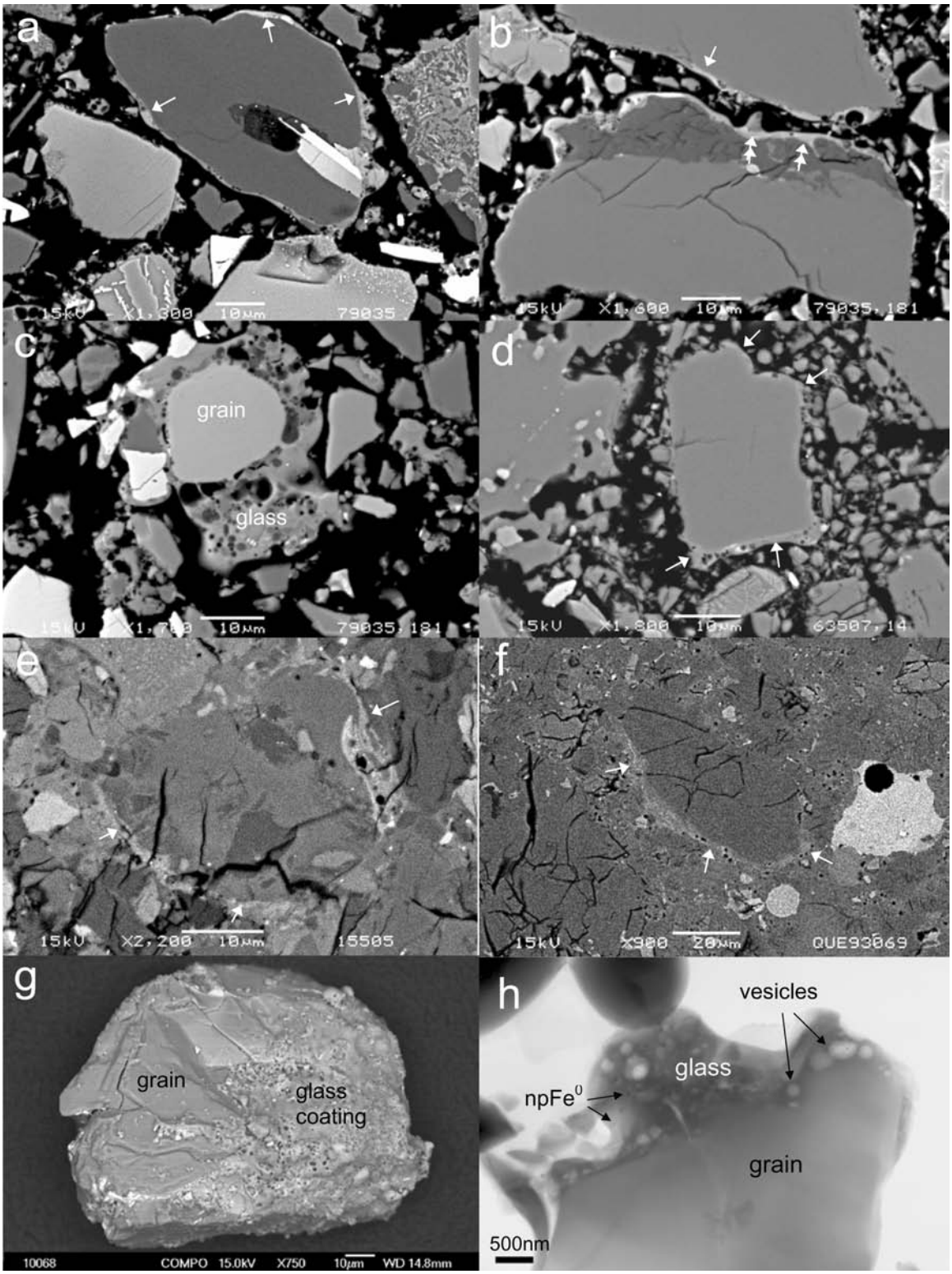

Fig. 10. Examples of glass rims: a) multi-lithic grain from 79035 completely incased in a glass rim; b) two grains from 79035 with glass rims (note especially the obvious flow textures highlighted by double arrows); c) a pyx grain from 79035 that is surrounded by vesicular glass with incorporated lithic components; d) a plagioclase grain from highland soil 63507; e) a plagioclase grain from 15505 with a nearly complete rim; f) a glass rim from QUE 93069; g) a plagioclase grain from the disaggregated 10068 (this grain is approximately two-thirds coated with glass); h) a TEM bright field image of a glass rim from 79035.

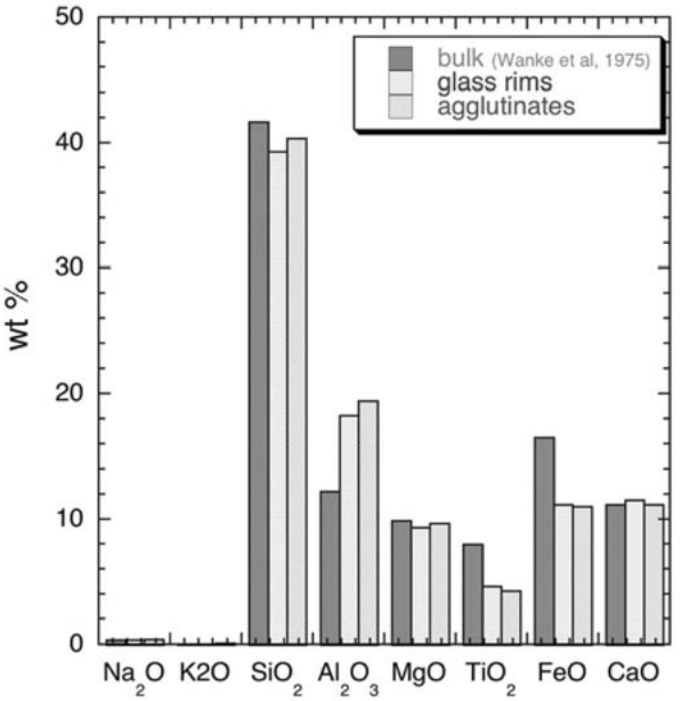

Fig. 11. Glass rims in 79035 are similar in composition to 79035 agglutinitic glass from the same thin section. Bulk data from Wänke et al. (1975).

Since glass rims are not seen in soils, they must also be created by the impact process in which the breccia was lithified. These rims have been identified on all scales from nanometer to millimeter and possibly even larger: for example, glass-coated pebbles have been found in terrestrial impact sites such as the Ries crater in Germany (French 1998). The exact mechanism of formation is still unknown, but the timing is clearly constrained. The "flow features," the general shape, and the 360° nature of the rims requires that the grains were free floating when the glass was acquired and thus the rims were acquired before being incorporated into the rock, perhaps in the ejecta curtain itself, or in a fluidized bed. The retention of solar flare tracks in the host mineral grains with glass rims indicates that the grains did not get hot enough to anneal the tracks.

IMPLICATIONS FOR REGOLITH BRECCIA METEORITES

Can our current meteorite collection provide information about space weathering and other regolith processes on asteroids? Regolith breccia meteorites from asteroidal parent bodies, like their lunar counterparts, are composed of regolith that has been lithified in impact. In order for us to reasonably expect to find space weathering products in asteroidal regolith breccia meteorites the following must be true: 1) conditions must exist now or have existed in the past on asteroid surfaces that are/were conducive for the formation of these products, and 2) parent body processes (e.g., lithification, transport) can not drastically alter these products so as to make them unrecognizable.

The environmental conditions at the asteroid belt are clearly different than the lunar environment. As they are further from the sun, there is less solar wind and therefore less sputtering. The impact rate of meteorites and micrometeorites in the asteroid belt is greater, but the velocity of impacts is much smaller, resulting in less melting and vaporization and therefore fewer space weathering products. Finally, the higher impact rate results in more comminution, further diluting any weathering products. All of these factors suggest that asteroids should produce significantly fewer space weathering products than the moon.

All materials exposed to the space environment will experience space weathering to some extent. There is certainly spectral evidence that space weathering is active on asteroids. For example, Galileo data indicates a reddening of Ida and Gaspra surface regolith with time (Chapman 1996). Binzel et al. (1996) report that among S-type near-earth asteroids, a continuum exists from bodies that spectrally resemble ordinary chondrites to those with classic S-type spectra, consistent with an ongoing alteration process. Some of the observed spectral changes (e.g., a "red" continuum at visible wavelengths) are similar to those seen in lunar soils (Pieters et al. 2000), so it is reasonable to infer that similar processes are involved producing comparable soil rims. Thus, the first condition is probably valid: the spectral evidence

Table 2. Comparison of the types of rims found in mature lunar soils and regolith breccias.

	Amorphous	NpFe^0-bearing	Glass	Vesicular
Lunar soil	common	abundant	absent	rare
Lunar regolith breccia	minor	common	abundant	abundant

indicates that space weathering products are currently created on asteroids. In order to account for the observed spectral changes, we estimate that vapor/sputter-deposited rims must be present on at least 1–5% of grains at the surface. Solar flare and cosmic ray data indicates that no more than ~20% of the grains in a typical meteoritic regolith breccia have been directly exposed at the surface (Macdougall 1981). Thus, weathering products are expected to be rare compared to the lunar case. However, they should be present in concentrations high enough that it would be statistically likely to find one or more rims in a typical TEM sample.

Based on our observations of space weathering products in lunar breccias of increasing grade, we suggest that weathering products (if formed) will be retained and preserved in meteorite breccias. While it appears that severe shock and compaction make finding weathering products more difficult, they can still often be identified. It is also true that there are many regolith breccia samples in the collection that have experienced only low levels of shock, and indeed, even samples which are classified as "friable."

CONCLUSIONS

The constituent grains within lunar regolith breccias show four distinct types of rims. Table 2 contains a summary of the type and abundance of these rims. Two of these rim types, amorphous and npFe^0-bearing, are indistinguishable from rims found in lunar soils and are clearly linked to soil processes. The other two rim types, vesicular and glass, are only rarely found in lunar soils despite being very common in regolith breccias. It is therefore concluded that these latter two types of rims are linked directly to the breccia-forming process.

Lunar regolith breccias retain much of the space weathering products acquired prior to and during their transformation into a lithified rock. Though these products may be modified by shock and compaction, they often still retain their characteristic features and can be readily recognized.

While we might expect soil rims to be much rarer in asteroidal regolith breccias, it should be possible to identify them if they are there. Pristine soil rims were identified in three of the four breccias examined. These rims are simply not easily destroyed. Only QUE 93069, the most highly shocked and recrystallized sample, contained no identifiable soil rims.

Glass rims, the most common type of rim found in lunar regolith breccias, are likely to also be the most common type of rim found in asteroidal regolith breccias. With the lower impact velocities on asteroids, melt should be significantly easier to create than vapor. Also, while soil and vesicular rims require TEM to observe, glass rims can be readily identified with SEM. This makes glass rims decidedly easier to find in general.

The formation of vesicular rims is still poorly understood, but it appears to be linked to solar-wind-implanted gases. As less solar wind reaches the asteroid belt and gardening times (the time it takes to turn over the soil) are shorter, one would expect less implanted gas than is seen at the moon. Impact temperatures should also be lower due to slower average impact velocities, in which case vesicular rims may be less common.

Regolith breccias retain a lot of history within them: the history of the impact event in which they were created, the history of the soil from which they were created, and the history of the rocks from which the soil was composed. Through careful examination of these lunar regolith breccias, we are learning to separate and interpret these very different but equally important histories.

Acknowledgments–This manuscript benefited greatly from thorough reviews by Natasha Johnson and John Bradley and from the editorial comments of Randy Korotev. NASA support (NGT9-66, SKN), (NAG5-11763, CMP), and (RTOP 344-31-40-07, LPK) is gratefully acknowledged.

Editorial Handling—Dr. Randy Korotev

REFERENCES

Basu A., Bogard D. D., Garrison D. H., Lauer H. V., Lindstrom D., McKay D. S., Morris R. V., Pieters C. M., and Wentworth S. J. 2000. A status report on the consortium study of regolith breccia 10068 (abstract #1941). 31st Lunar and Planetary Science Conference. CD-ROM.

Bernatowicz T. J., Nichols R. H., Hohenberg C. M., and Maurette M. 1994. Vapor deposits in the lunar regolith: Technical comment. *Science* 264:1779–1780.

Binzel R. P., Bus S. J., Burbine T. H., and Sunshine J. M. 1996. Spectral properties of near-Earth asteroids: Evidence for sources of ordinary chondrite meteorites. *Science* 273:946–948.

Bischoff A., Rubin A. E., Keil K., and Stöffler D. 1983. Lithification of gas-rich chondrite regolith breccias by grain boundary and localized shock melting. *Earth and Planetary Science Letters* 66: 1–10.

Borg J., Bibring J-P., Cowsik G., Langevin Y., and Maurette M. 1983. A model for the accumulation of solar wind radiation damage effects in lunar dust grains, based on recent results concerning implantation and erosion effects. 13th Lunar and Planetary Science Conference. pp. A725–A730.

Carrez P. Demyk K., Cordier P., Gengembre L., Grimblot J., D'Hendecourt L., Jones A. P., and Leroux H. 2002. Low-energy helium ion irradiation-induced amorphization and chemical

changes in olivine: Insights for silicate dust evolution in the interstellar medium. *Meteoritics & Planetary Science* 37:1599–1614.

Chapman C. R. 1996. S-type asteroids, ordinary chondrites, and space weathering: The evidence from Galileo's fly-bys of Gaspra and Ida. *Meteoritics & Planetary Science* 31:699–725.

Christie J. M., Griggs D. T., Heuer A. H., Nord G. L., Radcliff S. V., Lally J. S., and Fisher R. M. 1973. Electron petrography of Apollo 14 and 15 breccias and shock-produced analogs. 4th Lunar Science Conference. pp. 365–382.

Demyk K., Carrez P., Leroux H., Cordier P., Jones A. P., Borg J., Quirico E., Raynal P. I., and D'Hendecourt L. 2001. Structural and chemical alteration of crystalline olivine under low energy He^+ irradiation. *Astronomy and Astrophysics* 368:L38–L41.

Dran J. C., Durrieu L., Jouret C., and Maurette M. 1970. Habit and texture studies of lunar and meteoritic material with the 1 MeV electron microscope. *Earth and Planetary Science Letters* 9:391–400.

Fraundorf P., Flynn G. J., Shirck J., and Walker R. M. 1980. Interplanetary dust collected in the Earth's stratosphere: The question of solar flare tracks. 11th Lunar and Planetary Science Conference. pp. 1235–1249.

French B. M. 1998. *Traces of catastrophe*. Houston: Lunar and Planetary Institute. 120 p. http://www.lpi.usra.edu/publications/books/CB-954/CB-954.intro.html. Last accessed May 10, 2005.

Fruland R. M. 1983. *Regolith breccia workbook*. Houston: NASA. 269 p.

Hapke B. 2001. Space weathering from Mercury to the asteroid belt. *Journal of Geophysical Research* 106:10,039–10,073.

Heuer A. H., Christie J. M., Lally J. S., and Nord G. L. Jr. 1974. Electron petrographic study of some Apollo 17 breccias. 5th Lunar Science Conference. pp. 275–286.

Jowsiak D. J., Brownlee D. E., Schlutter D. J., and Pepin R. O. 2004. Experimental studies on heated and unheated He-irradiated olivine grains at moderate He-ion fluences: Analogues to radiation damage in IDPs (abstract #1919). 35th Lunar and Planetary Science Conference. CD-ROM.

Keller L. P. and Clemett S. J. 2001. Formation of nanophase iron in the lunar regolith (abstract #2097). 32nd Lunar and Planetary Science Conference. CD-ROM.

Keller L. P. and McKay D. S. 1993. Discovery of vapor deposits in the lunar regolith. *Science* 261:1305–1307.

Keller L. P. and McKay D. S. 1997. The nature and origin of rims on lunar soil grains. *Geochimica et Cosmochimica Acta* 61:2331–2341.

Lindstrom M. M., Mittlefehldt D. W., Morris R. V., Martinez R. R., and Wentworth S. J. 1995. QUE 93069, a more mature regolith breccia for the Apollo 25th anniversary (abstract). 26th Lunar and Planetary Science Conference. p. 849.

Macdougall J. D. 1981. Space exposure of breccia components. In *Workshop on lunar breccias and soils and their meteoritic components*, edited by Taylor G. J. and Wilkening L. L. Houston: Lunar and Planetary Institute. 94 p.

McKay D. S., Heiken G. H., Basu A., Blanford G., Simon S., Reedy R., French B. M., and Papike J. 1991. The lunar regolith. In *The lunar sourcebook*, edited by Heiken G. H., Vaniman D. T., and French B. M. New York: Cambridge University Press. pp. 284–356.

Nichols R. H. Jr., Hohenberg C. M., and Olinger C. T. 1994. Implanted solar helium, neon, and argon in individual lunar ilmenite grains—Surface effects and a temporal variation in the solar-wind composition (abstract). *Geochimica et Cosmochimica Acta* 58:1031.

Nier A. O. and Schlutter D. J. 1992. Extraction of helium from individual interplanetary dust particles by step heating. *Meteoritics* 27:166–173.

Noble S. K., Pieters C. M., and Keller L. P. 2001a. Can space weathering survive lithification? Results of a TEM study of lunar regolith breccia 10068 (abstract #1334). 33rd Lunar and Planetary Science Conference. CD-ROM.

Noble S. K., Pieters C. M., Taylor L. A., Morris R. V., Allen C. C., McKay D. S., and Keller L. P. 2001b. The optical properties of the finest fraction of lunar soil: Implications for space weathering. *Meteoritics & Planetary Science* 36:31–42.

Noble S. K., Keller L. P., and Pieters C. M. 2002. Understanding and identifying space weathering products in regolith breccias (abstract). *Meteoritics & Planetary Science* 37:A110.

Pieters C. M., Taylor L. A., Noble S. K., Keller L. P., Hapke B. H., Morris R. V., Allen C. C., McKay D. S., and Wentworth S. 2000. Space weathering on airless bodies: Resolving a mystery with lunar samples. *Meteoritics & Planetary Science* 35:1101–1107.

Pieters C. M. and Taylor L. A. 2003. Systematic global mixing and melting in lunar soil evolution. *Geophysical Research Letters* 30, doi:10.1029/2003GL019212.

Pieters C. M., Fischer E. M., Rode O., and Basu A. 1993. Optical effects of space weathering: The role of the finest fraction. *Journal of Geophysical Research* 98:20,817–20,824.

Sandford S. A. and Bradley J. P. 1989. Interplanetary dust particles collected in the stratosphere—Observations of atmospheric heating and constraints on their interrelationships and sources. *Icarus* 82:146–166.

Wänke H., Palme C., Baddenhausen H., Driebus G., Jagoutz E., Kreuse H., Palme C., Spettel B., Teschke F., and Thacker R. 1975. New data on the chemistry of lunar samples: Primary matter in the lunar highlands and the bulk composition of the Moon. 6th Lunar Science Conference. pp. 1313–1340.

Warren P. H. 2001. Porosities of lunar meteorites: Strength, porosity, and petrologic screening during the meteorite delivery process. *Journal of Geophysical Research* 106:10,101–10,111.

Wentworth S. J., Keller L. P., McKay D. S., and Morris R. V. 1999. Space weathering on the Moon: Patina on Apollo 17 samples 75075 and 76015. *Meteoritics & Planetary Science* 34:593–603.